IOSR Journal of Environmental Science, Toxicology and Food Technology (IOSR-JESTFT)
e-ISSN: 2319-2402,p- ISSN: 2319-2399.Volume 14, Issue 2Ser. IV (February. 2020), PP 24-33
www.iosrjournals.org

Bio-sorption of Methylene Blue and basic fuchsin from aqueous solution onto defatted *Carica papaya* seeds: mechanism and effect of operating parameters on the adsorption yield.

Aïssatou Alioune Gaye[1*], Nicolas Cyrille Ayessou[1,2]
[1]*Centre d'Études sur la Sécurité Alimentaire et Les Molécules Fonctionnelles (CESAM), École Supérieure Polytechnique*
[2]*Laboratoire d'Électrochimie et des procédés membranaires, École Supérieure Polytechnique*

Abstract:*The aim of the present work is to investigate the efficiency of the cationic dyes removal onto defatted Carica papaya seeds (DCPS). Batch mode experiments were performed for determining optimal parameters of dyes removal on the defatted seeds. The surface charge distribution of DCPS was determined and the point zero charge was found to be 6.4.The contact time for maximal adsorption capacities are found to be 180 mn for methylene blue (MB) and 150 mn for basic fuschin (BF). The removal capacities of both dyes increased rapidly from 93.23%to 97.21% for MB and 88.34% to 95.08 % when the pH varies between2and 3.The, it remains stable when varying the pH from 3 to 11. Dye concentrations (10 to 100 mg / L)do not influence the elimination capacities. The dye amounts adsorbed are dependent to mass of adsorbent doses. For the MB the adsorbent concentration value found for the maximum removal capacity is 8 g/L while the value is 6 g/L for the basic fuchsin. Various kinetics and adsorption isotherm models of the adsorption processes analyzed the adsorption mechanisms.The kinetics of the adsorption process were found to follow the pseudo-second-order rate law. Experimental values of the adsorption capacity reached the optimum values predicted by this model. The adsorption parameters were in good agreement with the Freundlich isotherm for MB and Temkin isotherm for BF.*

Keywords: *Dye,Isotherm, Kinetic, Carica, Adsorbent*

Date of Submission: 11-02-2020 Date of Acceptance: 27-02-2020

I. Introduction

Synthetic and natural dyes are widely used in chemical, pharmaceutical, textile and food factories and can cause dramatically environmental damages [1-3] and yield considerable wastewater quantities [4,5]. Wastewater polluted by organic dyes are difficult to purified, owing to the good stability of the aromatic structure of these compounds [6].Methylene blue (MB) is a cationic dye extensively used in industry with a recalcitrant nature. This dye is toxic and causes several environment and health risks. Hemolytic anemia, hyberbilirubinemia, and acute renal failure, have been reported as consequence of the exposure of neonate to methylene blue [7]. Basic fuchsin (BF) is a cationic dye widely used in textile and leather industries. Exposure to basic fuchsin may cause drastically damage to health such as irritation to the respiratory tract, severe eye and skin irritation, nausea, vomiting and diarrhea [8]. Damages to thyroid, liver and spleen are also reported [9,10]. Removal of these dyes from wastewater is essential for both health and environmental aspects. Traditional wastewater treatment technologies proven ineffective for purifying wastewater polluted by some types of dye [11]. Several methods were used for removal dye from wastewater. Implementation of physico-chemical and biological processes such as membrane separation [12], oxidation [13], osmosis [14], photodegradation[15], microbial biodegradation [16-18] are difficult and are expensive. Some of these processes have a main disadvantage owing to the formation of unknown compounds different to the original dye molecule [19,20]. These intermediates may have different toxicity [21] and remain in solution after the treatment of the polluted water. The adsorption method is the easiness and the low-cost process compared to the other processes used in industry. A large number of adsorbents such as nanoparticles, clays, zeolites, byproduct of cellulose, activated carbon, agro-industrial wastes are applied for removing dyes from wastewater [22,23]. The adsorption process is also the most efficient technology for removal dye from wastewater. No intermediates issued from the degradation of the dye molecules appeared because the dye molecules directly transferred from the solution to the solid phase of the adsorbent. In addition, the amounts of adsorbent used are quite low. At the end of the process, the adsorbent loaded dye can be stored in dry phase without damage for environment. The solid phase can be regenerated later to be reused in the process.

In this context, we proposed the use of the residue of the defatted *Carica* papaya seed (DCPS), which is very low-cost adsorbent removal dye (MB and BF, scheme 1) from wastewater. The biosorption mechanisms of

these dyes on the defatted seed were studied by determining the influence of parameters such as pH, concentration, ratio dye/absorbent and time contact. The equilibrium and the kinetic data of the adsorption process of the two dyes on the DCPS were also examined.

II. Material And Methods

2.1 Preparation of the adsorbent

Red Lady *Carica* papaya L. was harvested at the Sébikhotane protected forest (region of Dakar in Senegal 14˚43'14.4"N, 17˚08'16.4"W). The non-defatted *Carica* papaya seed (CPS) collected from mature fruits thoroughly washed with distillated water and air shadow dried for three days. After this process, the CPS were dried at 45°C during 48 hours. Finely the non-defatted seed were ground using a grinder and defatted with hexane in order to obtain the defatted CPS(DCPS). Then itwas air-dried, milled, sieved to an average particle of 0.25 mm and stored in a plastic container.

2.2 Point zero charge pH_{PZC}

The pH of the point of zero charge (pH_{PZC}) for the DCPS was determined by a titration procedure. To a series of eleven 150 mL conical flasks 45 mL of a solution of KNO_3 0.01 M were added and the pH was accurately adjusted using HCl or NaOH 0.01 N solutions from pH = 2 to pH = 12 and completed with a solution KNO_3 0.01 M to 50 mL. The initial pH (pH_i) was accurately measured again. To each flask, 0.1 g of DCPS was added and the flask was capped and shaken manually each 4 hours. After 48 hours, the final pH (pH_f) was measured. The $\Delta pH = pH_f - pH_i$ is plotted against pH_i. The point of intersection of the curve and the abscissa axe at $\Delta pH = 0$ gave the pH_{PZC}.

2.3 Batch adsorption tests

All the experiments were conducted in discontinuous batches. A **weighed sample** of DCPS was mixed with a 50 mL dye solution in 250 mL conical flasks and the constant agitation was maintained for a fixed time at 25°C. At the end of the operation, the liquid phase was separated from the adsorbent by filtration through a Whatmanfilter N°4. The residual dye concentration in liquid was determined by measuring the absorbance of the solution at specific wavelengths (λ_{max} =663.5nm for MB and λ_{max} = 517.1 nm for BF) using spectrophotometer (Lambda, Perkin Elmer). The experimental data were used to calculate the removal capacity and the quantity of dye adsorbed on the DCPS.

$$Removal\ capacity\ (\%) = \frac{(C_0 - C_e)\cdot \mathrm{V}}{C_0} \times\ 100$$

$$q_e = \frac{(C_0 - C_e)\cdot \mathrm{V}}{m_0}$$

where C_0 and C_e are respectively the initial and the final dye concentrations (mg/L) in the liquid phase, V (L) is the volume of the liquid phase and m_0 (g) is the adsorbent mass used.

2.4 Effect of the time contact

The equilibrium time was determined using a concentrated dye solutions of 50 mg/L (BF and MB). Then 50 mL of each dye solution was treated with 0.25 g of adsorbent at time ranging from 10 to 180 mn. The experiments were conducted at the same pH and the flasks were shaken at 500 rpm and at temperature of 25°C.

2.5 Effect of solution pH on the removal capacity

The effect of solution pH on the dyes removal capacities of the adsorbent was investigated between pH = 2 and pH = 11. The experiments were performed by adding a 0.4 g of DCPS powder into six 150 mL conical flasks containing 50 mL of 50 mg L^{-1} dye solutions and the pH of the solution was adjusted using 0.1 N HCl or 0.1 N NaOH. The flasks were shaken at 500 rpm and at temperature of 25°C for 180 mn.

2.6 Effect of adsorbent dose on the removal capacity

The effect of the adsorbent dose was studied using the following procedure. 50 mL of dye solution of 50 mg/L concentration was treated with a mass of adsorbent ranging from 0.1 to 2 g. The experiments are conducted at the same pH and the flasks were shaken at 500 rpm and at temperature of 25°C for 180 mn.

(A)(B)

Scheme 1. The chemical structures of the tested dyes where (A) is methylene blue and (B) is basic fuchsin.

2.7 Statistical analysis

All the measurements were carried out in triplicate. The mean values and standard deviations were calculated and the data were expressed as mean ± SD. Xlstat 2019 software was used for the data and statistical analysis. Differences were considered significant at the $p < 0.05$ level based on Duncan's new multiple range test.

III. Results and discussion

3.1 Infrared spectra

The FT-IR (Figure1) of the CPS, DCPS, MB-loaded DCSP and BF-loaded DCSP, were recorded on the Perkin Elmer spectrophotometer Two in the range 4000 – 400 cm^{-1}. In the spectra of DCPS, the broad band pointed at *ca*. 3280 cm^{-1} is characteristic of the vibration of an associated –OHgroup[24]. On comparison the CPS spectra shows two bands attributable to –OH group at 3675 cm^{-1} and 3287 cm^{-1}. The –OH group is present in phenolic and carboxylic moieties. The band at 3675 cm^{-1} can also be attributed to the water molecules adsorbed on the surface of the solid CPS. For DCPS, bands with weak intensities located in the range 2850–2800 cm^{-1} are due to the stretching and bending modes of the –CH of the methylene and the methyl groups. For CPS intense bands appear in the region 2925–2860 cm^{-1} due to –CH of the skeletons present in lipids, cellulose, hemicellulose and lignin structures. The intense band pointed in the spectrum of DCPS at *ca*. 1634 cm^{-1} is due to theC=O [25]. The non-defatted CPS present a very intense band at *ca*. 1745 cm^{-1} and a medium band at *ca*. 1635 cm^{-1}. These two bands are due to the presence of tri-ester before defatting of seeds. The bands located in the range 1600–1400 cm^{-1} are attributed to the C=C in aromatic rings. Multiple vibrations due to the C–O moiety attributed to phenol are pointed in the region 1285–1000 cm^{-1}. This splitting pattern is indicative of the presence of different types of phenols[26]. All changes in intensity and position in the FT-IR peaks of dye-loaded-DCPS verify that different functional groups present in DCPS are involved in dye ion binding. Additionally the FT-IR spectra of dye-loaded-DCPS show bands characteristic of MB and BF respectively.

3.2 Optimization of adsorption parameters

The point of zero charge of DCPS (Figure 2) was determined. The time contact is the first parameter studied because of the important role it plays in the equilibrium of the adsorption. As shown in Figure 3a, at t = 10 min a high removal capacity is observed: 94.62 % for MB and 82.79 % for BF. When increasing time contact the removal capacity increase very slowly and stabilize at 97.85% for MB and 93.60 % for BF at t = 180 min. In the continuation of the work the time of contact is fixed at t = 60 min. The rapid adsorption rate of dyes is probably due to the large number of unoccupied adsorption sites on the surface of the adsorbent. The rate of adsorption is drastically reduced after t = 10 min owing to the low number of unoccupied sites remaining on the surface area of the adsorbent and the repulsive force induced by the adsorbed dye molecules [27,28].

The second parameter studied is the pH (Figure 3b). The influence of the pH on the removal dye capacities is significant because of its effect on the surface of the adsorbent and on the protonation or deprotonation of the dye molecules [29]. When the pH of the solution is superior to the pH_{PZC}, which is the value of pH at which the charge of adsorbent surface is zero, the surface of the adsorbent is negatively charged and the cationic dye molecules are easily fixed by the adsorbent. In contrary when the pH of the solution is inferior to the pH_{PZC}, the surface of the adsorbent is positively charged and the cationic dye molecules interact less easily with the adsorbent [30].The removal capacities of dyes are lower in acidic media: 93.23 % for MB and 88.34 % for BF when pH = 2.2.

The low removal capacity in acidic solution can be explained by the competition between the cationic dye and the H^+ ions. In fact the H^+ ions can be adsorbed on the adsorbent surface and the consequence is the diminution of the number of active sites available for the adsorption of cationic dye molecules. The removal capacities remain quasi-constant when the pH increases from 3 to 11: 97.21-97.42 % for MB and 95.05-95.94 %

for BF. The maximum is reached for a pH = 9 for MB and for a pH = 11 for BF (Figure 3b). When increasing pH, the number of H^+ ions decreases rapidly, the competition with dye molecules disappears and the number of adsorption sites available for dye molecules increases.

The third effect studied is the influence of the adsorbent dose on the removal capacity (Figure 3c). Adsorbent mass used is in the range 0.1 to 1 g and fixing the initial concentration of the dye at 50 mg/l and the time contact at 60 min. The pH of the solution is superior to the pH_{PZC}.The highest removal capacity is observed at 0.4 g with 97.44 % of MB removal and at 0.3 g with 96.70 % of BF removal. It is observed that for both dyes the removal capacities is adsorbent-dose dependent: 93.58-97.44 % for MB and 95.7-96.7 % for BF. This fact could be explained by the increase of the adsorbent surface areas, which are compatible with the augmentation of the number of adsorption sites available for the dye molecules.

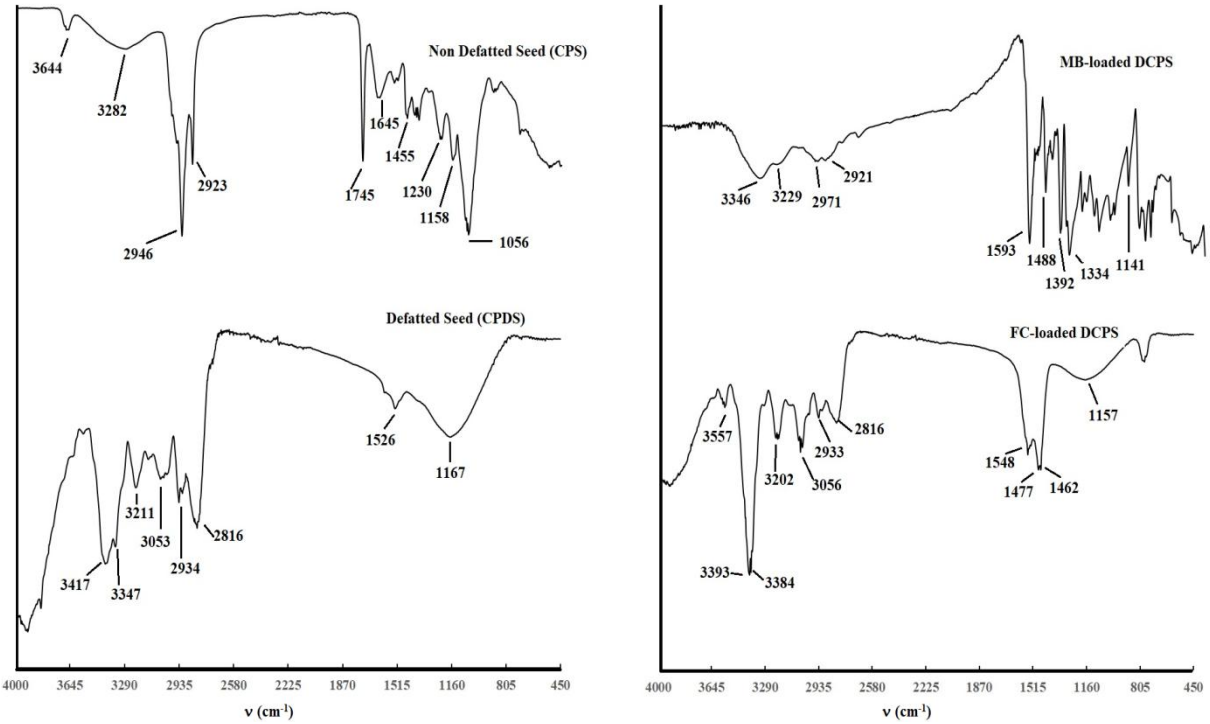

Figure 1: FT-IR spectra of *Carica* papaya non-defatted seed (a), defatted *Carica* papaya seed (DCPS) (b) MB-loaded DCSP (c), BF-loaded DCSP (d).

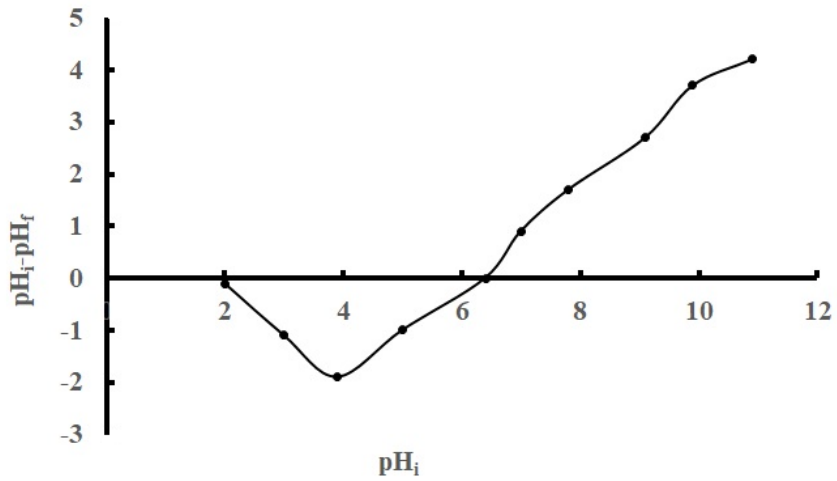

Figure 2:Determination of the point of zero charge of DCPS.

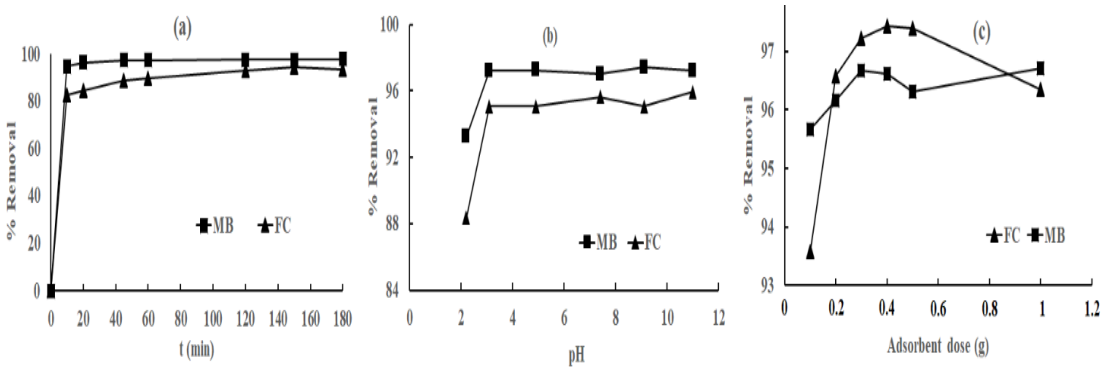

Figure 3:Parameters optimization for dyes removal: (a) Duration; (b) pH; (c) adsorbent dose.

3.3 Kinetics aspects

The kinetics studies of MB and BF on DCPS were carried out at pH = 7, temperature of 25°C and a fixed concentration of adsorbent 8 g/L for MB and 6 g/L for BF. Different initial dyes concentrations were used (25 ppm to 100 ppm). The aqueous concentrations of dyes were measured similarly, varying time contact. The amount of dye adsorbedq_t (mg/g) at time t is calculated using the following equation 1

$$\text{Equation 1: } q_t = \frac{(C_0 - C_t)\cdot V}{m_0}$$

where C_t (mg/L) is the aqueous dye concentration at time t, C_o (mg/L) is the initial concentration of dye, V is the volume (L) and m_0 (g) is the weight of adsorbent. Four kinetic models: pseudo-first-order [31], pseudo-second-order [32], intra-particle diffusion model [33] and Elovich model [34](Table 1) were examined in order to understand the adsorption mechanism on DCPS . The fit of these models was checked by each linear plot of the representative equation respectively (Figures 4 and 4') and by comparing to the regression coefficients for each expression. All the parameters of each model are presented in Table 1.

3.3.1 Pseudo-first-order model

The pseudo-first-order model, described by Equation 2, allows estimating the adsorption performance of the adsorbent from the aqueous solution of the adsorbate. This model assumes that the number of sites occupied by the adsorbed molecules is proportional to the number of free active sites.

$$\text{Equation 2:} \ln(q_e - q_t) = lnq_e - k_1 t$$

Whereq_e is the equilibrium adsorption quantity (mg/g), $q_t$is the amount of dye adsorbed at time t (mg/g), and k_1 is the rate constant (mn^{-1}).

On plotting the Equation 2 (Figure 4 (a and a')), the parameters $q_{e,cal}$, k_1 and R^2 were calculated and reported in Table 1 for both dyes. The $q_{e,cal}$values don't fit the experimental $q_{e,exp}$ values and the R^2 values are very low. These facts are indicative of the pseudo-first-order model is not applicable to the process.

3.3.2 Pseudo-second-order model

The model is described by the Equation 3 and assumes that the number of occupied sites is function of the square of the number of free active sites on the adsorbent.

$$\text{Equation 3:} \frac{t}{q_t} = \frac{1}{k_2 q_e^2} + \frac{t}{q_e}$$

On plotting the Equation 3 (Figure 4 (b and b')), straight lines are observed for MB and BF dyes at different initial dyes concentrations (25 mg/L to 100 mg/L). The parameters $q_{e,cal}$, k_2 and R^2 were calculated and reported in Table 1 for both dyes. The $q_{e,cal}$values fit the experimental $q_{e,exp}$ values and the R^2 values are close to the unit. These facts are indicative that the pseudo-second-order model describes the process very well for both dyes MB and BF.

3.3.3 Intra-particle diffusion model

The Intra-particle diffusion model is described by the Equation 4.

$$\text{Equation 4:} q_t = k_i t^{1/2} + I$$

As reported in the literature [35] the plot of Equation 4 should be linear if intra-particle diffusion is involved in the adsorption mechanism. Additionally intra-particle diffusion is the rate-controlling step, if the straight line passes through the origin. If the straight line does not cross the origin, this is indicative that the intra-particle is not the only rate-controlling step. Figure 4 (c and c') shows the plots of Equation 4for MB and BF dyes at different initial dyes concentrations (25 mg/L to 100 mg/L). All curves are linear and do not pass though the origin and the correlation coefficients R^2 are low. These observations are indicative that the intra-particle diffusion in not the only rate-controlling step and it operate in both cases simultaneously with the pseudo-second-order model [36].

3.3.4 Elovich model

The kinetic model named Elovich, illustrated by the mathematical Equation 5, describes the chemisorption on heterogenous surfaces.

$$\text{Equation 5: } q_t = \frac{1}{\beta}\ln(\alpha\beta) + \frac{1}{\beta}\ln t$$

whereq_t is the amount of dye adsorbed (mg/g) at time (t), α represents the initial sorption rate (mg g^{-1} min^{-1}) and β is related to the extent of surface coverage and activation energy for chemisorption (g mg^{-1}). On plotting Equation 5 (Figure 4 (d and d')) straight lines are observed for both dyes for the different initial concentrations. The parameters α, β and the correlation coefficients $R^2$are calculated from the linear plots and consigned in Table 1. The whole correlation coefficients were lower than the unit. This model is not suitable to study the sorption of MB and BF on DCPS.

The sorption process of MB and BF on DCPS is complex and involves more than one mechanism. It is best described by the pseudo-second-order model as shown by the parameters values tabulated in Table 1. Intraparticle diffusion, which is not the rate-controlling step, is also involved in the mechanism of sorption.

Table 1: Kinetic parameters for adsorption of MB and BF on DCPS.

Dye	C_0 (mg/L)	$q_{e,exp}$ (mg/g)	Pseudo-first-order model kinetic			Pseudo-second-order model kinetic			Intra-particle diffusion model			Elovich kinetic model		
			$\ln(q_e - q_t) = \ln q_e - k_1 t$			$\frac{t}{q_t} = \frac{1}{k_2 q_e^2} + \frac{1}{q_e} t$			$q_t = k_i t^{1/2} + I$			$q_t = \frac{1}{\beta}\ln \alpha\beta + \frac{1}{\beta}\ln t$		
			k_1 (mn^{-1})	$q_{e,cal}$ (mg/g)	R^2	k_2 (g/mg/mn)	$q_{e,cal}$ (mg/g)	R^2	k_i (mg/g/mn)	I	R^2	β (g/mg)	α (mg/min)	R^2
MB	25	3.06	0.0332	0.058	0.4401	1.9975	3.0619	0.9999	0.0117	2.9724	0.6535	35.5872	3.26×10^{45}	0.7453
	50	6.10	0.0302	0.032	0.4125	4.5586	6.0976	1.0000	0.0087	6.034	0.6733	46.7290	1.015×10^{122}	0.8018
	75	9.13	0.0276	0.117	0.8324	1.1850	9.1408	1.0000	0.0243	8.9573	0.8139	17.3913	1.074×10^{67}	0.8991
	100	12.17	0.0895	0.283	0.9916	0.6987	12.2100	1.0000	0.0356	11.936	0.8999	11.9617	3.993×10^{61}	0.9786
BF	25	2.98	0.0401	0.0388	0.6955	20.4777	2.9797	1.0000	0.0045	2.9498	0.4067	88.4955	8.04×10^{112}	0.504
	50	6.01	0.0531	0.0554	0.263	1.6701	6.0241	1.0000	0.0168	5.8988	0.5833	24.0963	10.81×10^{61}	0.7026
	75	9.01	0.1350	0.5324	0.9511	0.5446	9.0744	1.0000	0.0582	8.6516	0.7744	7.0872	1.59×10^{26}	0.9002
	100	12.00	0.1363	1.2672	0.9704	0.2164	12.1507	1.0000	0.1318	11.182	0.7986	3.1427	6.77×10^{14}	0.9191

Table 2: Isotherm parameters for adsorption of MB and BF on DCPS.

Dye	Langmuir isotherm $\frac{C_e}{q_e} = \frac{1}{K_L Q_0} + \frac{C_e}{Q_0}$			Freundlich isotherm $logq_e = logK_F + \frac{1}{n} logC_e$			Temkin isotherm $q_e = B\ logK_T + B\ logC_e$		
	Q_0 (mg/g)	K_L (L/mg)	R^2	1/n	K_F	R^2	B (J/mol)	K_T *(L/mole)*	R^2
MB	42.372	0.145	0.8373	0.829	5.34	0.9981	5.278	3.1917	0.9426
BF	-14.92	-0.123	0.4130	1.3608	2.0739	0.9546	7.033	1.321	0.9912

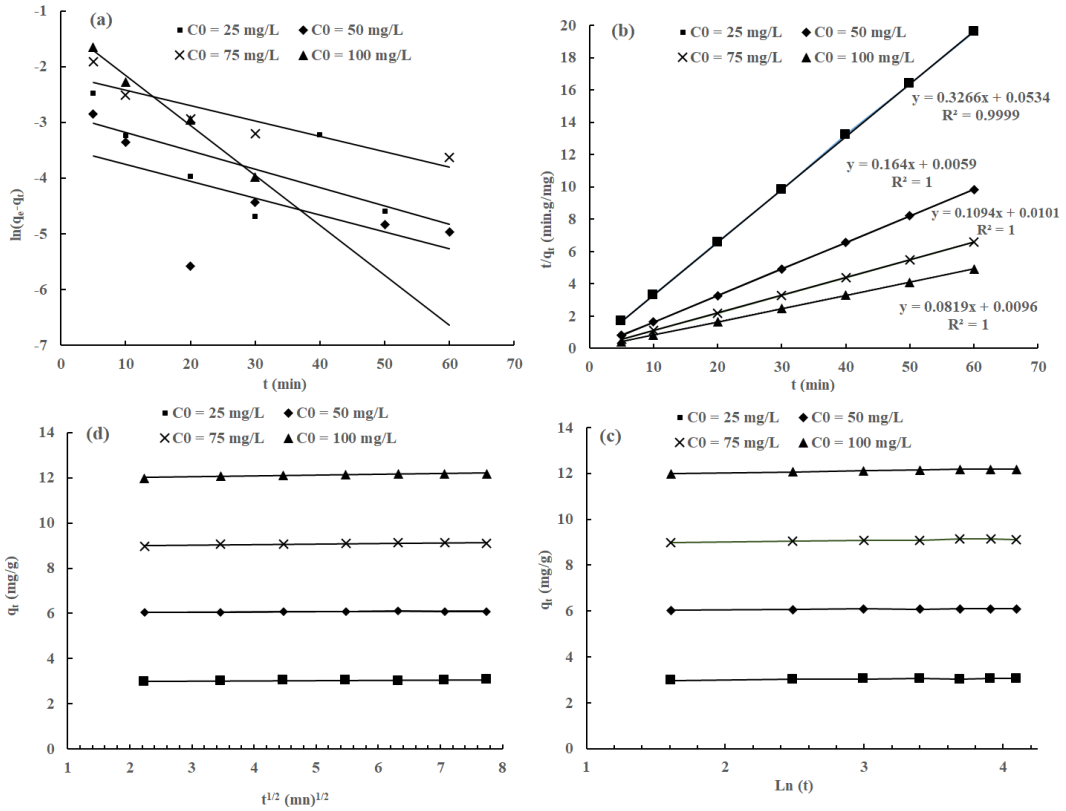

Figure 4 (a-d): Kinetics models for adsorption of MB on DCPS: pseudo-first order (a); pseudo-second order (b); intraparticle (c) and Elovich (d).

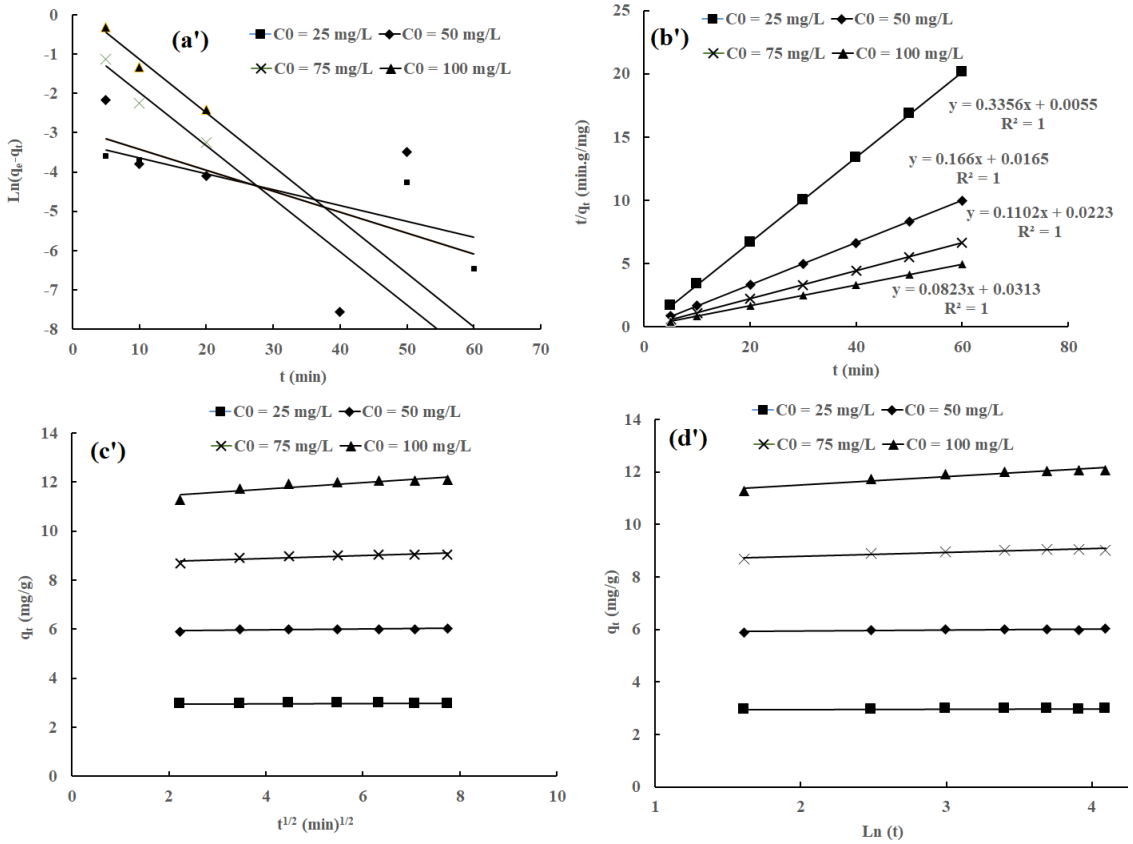

Figure 4(a'-d'):Kinetics models for adsorption of MB on DCPS: pseudo-first order (a); pseudo-second order (b); intraparticle (c) and Elovich (d).

3.4 Isotherm

For understanding how the adsorbed molecules are distributed between the liquid phase and the solid phase, which is constituted by the adsorbent, adsorption isotherms are studied at equilibrium. The experimental data are analyzed by fitting them with different models. For finding the best model for design purpose, isotherms models named Langmuir, Freundlich and Temkinwere used in this study [37].

The Langmuir model assumed that the adsorbent has specific homogeneous active sites. This model suggests that when a site is occupied, there can no longer be adsorption on this site. All the sites are energetically equivalent and there is no interaction between the adsorbed molecules on the neighboring sites. It is a monolayer sorption on homogeneous active sites and can be expressed by equation 6.

Equation 6: $\frac{C_e}{q_e} = \frac{1}{K_L Q_0} + \frac{C_e}{Q_0}$

On the other hand, in the Freundlich model, it is assumed that the surface of the adsorbent is heterogeneous with a non-uniform distribution of adsorption heat on the surface. This model suggests a multilayer sorption with non-equivalent sites that are associated with adsorption energies resulting from the interaction between the adsorbed species.

Equation 7: $logq_e = logK_F + \frac{1}{n}\ logC_e$

The Temkin model is more particularly used for the determination of the adsorption energy variation. The Temkin isotherm assumes that the decrease in sorption heat is linear. The Temkin isotherm can be expressed in the following linear form as in Equation 8.

Equation 8: $q_e = BlogK_T + BlogC_e$

Figures 5 and 6 represent the different linearized isotherms such as Langmuir, Freundlich and Temkin for MB and FC respectively. The estimated parameters (Q_0, K_L, *1/n*, K_F, *B* and K_T) of the whole isotherms are summarized in Table 2. The correlation coefficient values of R^2, which are important for estimating the goodness of fit, are also reported in Table 2.

The data in Table 2 show that the MB and BF does not follow the same model. Langmuir model was the poorest to fit the experimental adsorption equilibrium data for both dye. The correlation coefficient R^2 are so low with values of 0.8373 for MB and 0.4130 for BF. Experimental data of MB were fitted by Freundlich model with a very good correlation coefficient value of 0.9981. The adsorption is a multilayer adsorption process on heterogeneous sites. Interactions between adsorbed molecules occur, resulting in different energies of the adsorption reaction. The n value of 1.206 is indicative of a multimolecular adsorption mechanism. The K_F value of 5.34 indicates that the uptake of MB is not very easy, compared to the results obtained with MB when maize stem tissue is used as adsorbent. In this case, the K_F vary in the range 10-320 according to the pH of the solution[38]. For BF, the Temkin model was found to be the best model for fitting the experimental data, showing very good correlation coefficient value of 0.9912.

IV. Conclusion

In this study, DCPS was successfully used to clean water containing MB or BF. The elimination of these two dyes does not depend on the pH and is maximum for a contact time of 180 min. Adsorption kinetics are described for both dyes by the pseudo-second order model. The equilibrium of MB adsorption on DCPS is suitably described by the Freundlich model, while BF's one is best described by the Temkin model. These observations led to the conclusion that defatted papaya seed residue could be used as a potential adsorbent to remove MB and BF from an aqueous solution. This material, which has no financial value and considered as a waste of the papaya industry, has the potential for recovering in the treatment of wastewater from certain types of industries.

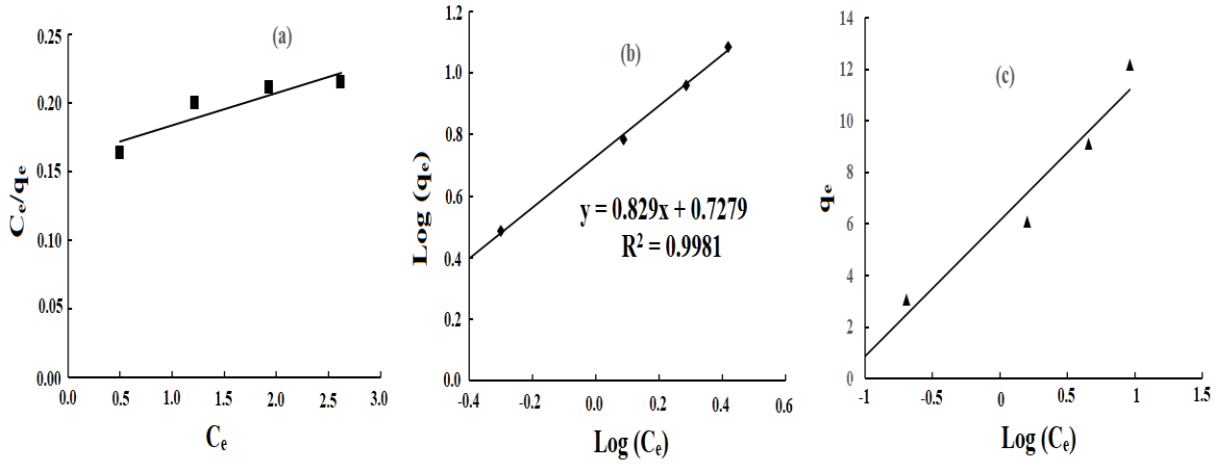

Figure 5: Isotherms for MB. Langmuir (a); Freundlich (b); Temkin (c).

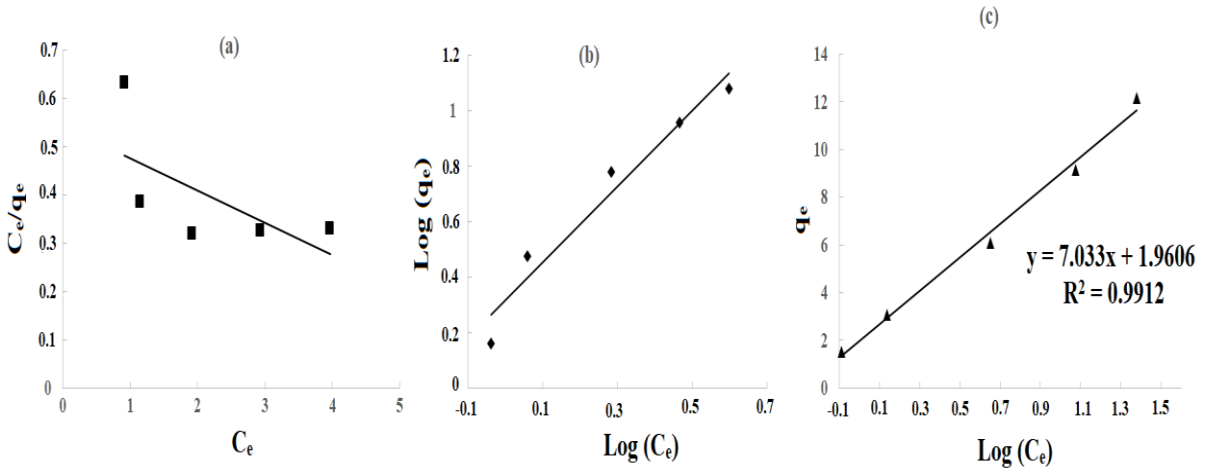

Figure 6: Isotherms for BF. Langmuir (a); Freundlich (b); Temkin (c).

References

[1]. T.-H.Kim, C.Park, S.Kim, Water recycling from desalination and purification process of reactive dye manufacturing industry by combined membrane filtration. J. Cleaner Prod. 13(8), 2005, 779–786.

[2]. A.N.Babu, D.S. Reddy, P.Sharma, G.S.Kumar, K. Ravindhranath G.V.K.Mohan, Removal of Hazardous Indigo Carmine Dye from Waste Water Using Treated Red Mud. Mater. Today: Proc., 17, 2019,198–208.

[3]. R. Khan, V. Patel, Z. Khan, Bioremediation of dyes from textile and dye manufacturing industry effluent.In: Singh, P. Kumar, A. Borthakur, A. eds. Abatement of Environmental Pollutants. Elsevier, 2020,107–125.

[4]. D.T. Sponza, Toxicity studies in a chemical dye production industry in Turkey. J. Hazard. Mater., 138 (3), 2006, 438–447.

[5]. V. Katheresan, J. Kansedo, S.Y. Lau, Efficiency of various recent wastewater dye removal methods: A review. J. Environ. Chem. Eng., 6(4), 2018, 4676–4697.

[6]. E. Forgacs, T. Cserháti, G. Oros, Removal of synthetic dyes from wastewaters: a review. Environ. Int., 30(7), 2004, 953–971.

[7]. M.Albert, M.S. Lessin, B.F. Gilchrist, Methylene blue: dangerous dye for neonates. J. Pediatr. Surg., 38(8), 2003, 1244–1245.

[8]. J.W. Churchman, The reverse selective bacteriostatic action of acid fuchsin. J. Exp. Med., 37(1), 1923, 1–10.

[9]. V.K. Gupta, A. Mittal, V. Gajbe,J. Mittal, Adsorption of basic fuchsin using waste materials bottom ash and deoiled soya as adsorbents, J. Colloid Interface Sci., 319(1), 2008,30–39.

[10]. L.A.Crandall, E. Oldberg, A.C. Ivy, Contributions to the physiology of the pancreas. Am. J. Physiol.-Legacy Content, 89(1), 1929, 223–229.

[11]. G.M.Shaul,T.J.Holdsworth,C.R. Dempsey, K.A. Dostal, Fate of water soluble azo dyes in the activated sludge process. Chemosphere, 22(1), 1991, 107–119.

[12]. J.He, A. Cui, S. Deng, J.P. Chen, Treatment of methylene blue containing wastewater by a cost-effective micro-scale biochar/polysulfone mixed matrix hollow fiber membrane: Performance and mechanism studies. J. Colloid Interface Sci., 512, 2018, 190–197.

[13]. H. Akrout, S. Jellali,L. Bousselmi, Enhancement of methylene blue removal by anodic oxidation using BDD electrode combined with adsorption onto sawdust. C. R. Chim., 18(1), 2015, 110–120.

[14]. E.W. Tow, M.M. Rencken,J.H. Lienhard, In situ visualization of organic fouling and cleaning mechanisms in reverse osmosis and forward osmosis, Desalination, 399, 2016, 138–147.

[15]. M.Naushad, G. Sharma, Z.A. Alothman, Photodegradation of toxic dye using Gum Arabic-crosslinked-poly(acrylamide)/$Ni(OH)_2$/FeOOH nanocomposites hydrogel. J. Cleaner Prod. , 241, 2019,118263.

[16]. V.Bharti, K.Vikrant, M.Goswami, H.Tiwari, R.K.Sonwani, J.Lee, D.C.W.Tsang, K.-H.Kim, M.Saeed, S.Kumar, B.N. Rai,B.S. Giri, R.S. Singh, Biodegradation of methylene blue dye in a batch and continuous mode using biochar as packing media. Environ. Res., 171, 2019, 356–364.
[17]. Z. Aksu, G. Karabayır, Comparison of biosorption properties of different kinds of fungi for the removal of Gryfalan Black RL metal-complex dye. Bioresour. Technol., 99(16), 2008, 7730–7741.
[18]. K. Vijayaraghavan, Y.-S. Yun, Bacterial biosorbents and biosorption. Biotechnol. Adv., 26 (3), 2008, 266–291.
[19]. Z.Mengting, T.A.Kurniawan, S.Fei, T.Ouyang, M.H.D.Othman, M.Rezakazemi,S. Shirazian, Applicability of $BaTiO_3$/graphene oxide (GO) composite for enhanced photodegradation of methylene blue (MB) in synthetic wastewater under UV–vis irradiation. Environ. Pollut., 255,2019, 113182.
[20]. S. Su, Y. Liu, X. Liu, J. Wei, Y. Zhao, Transformation pathway and degradation mechanism of methylene blue through β-FeOOH@GO catalyzed photo-Fenton-like system. Chemosphere, 218, 2019, 83–92.
[21]. S. Malato,P. Fernández-Ibáñez,M.I. Maldonado,J. Blanco,W. Gernjak, Decontamination and disinfection of water by solar photocatalysis: Recent overview and trends. Catal. Today, 147(1),2009, 1–59.
[22]. A.Bhatnagar, M. Sillanpää, Utilization of agro-industrial and municipal waste materials as potential adsorbents for water treatment: a review. Chem. Eng. J., 157(2), 2010, 277–296.
[23]. B.Royer, N.F.Cardoso, E.C.Lima, J.C.P.Vaghetti, N.M.Simon, T.Calvete, R.C. Veses, Applications of Brazilian pine-fruit shell in natural and carbonized forms as adsorbents to removal of methylene blue from aqueous solutions: Kinetic and equilibrium study. J. Hazard. Mater., 164(2), 2009, 1213–1222.
[24]. K.K.Krishnani, X.Meng, C.Christodoulatos, V.M.Boddu, Biosorption mechanism of nine different heavy metals onto biomatrix from rice husk. J. Hazard. Mater., 153(3), 2008, 1222–1234.
[25]. C.R.T.Tarley, M.A.Z. Arruda, Biosorption of heavy metals using rice milling by-products. Characterization and application for removal of metals from aqueous effluents. Chemosphere, 54(7), 2004, 987–995.
[26]. E.C. Lima, B. Royer, J.C.P. Vaghetti, N.M. Simon, B.M. da Cunha, F.A. Pavan, E.V. Benvenutti, R.C.Veses, C. Airoldi, Application of Brazilian pine-fruit shell as a biosorbent to removal of reactive red 194textile dye from aqueous solution: Kinetics and equilibrium study. J. Hazard. Mater., 155(3), 2008,536–550.
[27]. W.H.Mahmoud, N.F. Mahmoud, G.G. Mohamed, Mixed ligand complexes of the novel nanoferrocene based Schiff base ligand (HL): Synthesis, spectroscopic characterization, MOE studies and antimicrobial/anticancer activities. J. Organomet. Chem., 848, 2017,288–301.
[28]. Z.Hosseinabadi-Farahani, N.M. Mahmoodi, H. Hosseini-Monfared, Preparation of surface functionalized graphene oxide nanosheet and its multicomponent dye removal ability from wastewater. Fibers Polym., 16(5), 2015,1035–1047.
[29]. S.V.Mohan, N.C.Rao, J. Karthikeyan, Adsorptive removal of direct azo dye from aqueous phase onto coal based sorbents: a kinetic and mechanistic study. J. Hazard. Mater., 90(2), 2002, 189–204.
[30]. J.A.Schwarz, C.T.Driscoll, A.K. Bhanot, The zero point of charge of silica alumina oxide suspensions. J. Colloid Interface Sci., 97(1), 1984, 55–61.
[31]. Y.-S. Ho, Comments on using of 'pseudo-first-order model' in adsorption [Int. J. Biol. Macromol. vol. 81]. Int. J. Biol. Macromol., 88, 2016, 505–506.
[32]. J.-P. Simonin, On the comparison of pseudo-first order and pseudo-second order rate laws in the modeling of adsorption kinetics. Chem. Eng. J., 300, 2016, 254–263.
[33]. K. Anbalagan, M.M.Kumar,K. Ilango, R.Mohankumar, R.L. Priya, Prelusive scale extraction of mangiferin from Mangifera indica leaves: Assessing solvent competency, process optimization, kinetic study and diffusion modelling. Ind. Crops Prod., 140, 2019, 111703.
[34]. F.-C.Wu, R.-L.Tseng, R.-S. Juang, Characteristics of Elovich equation used for the analysis of adsorption kinetics in dye-chitosan systems. Chem. Eng. J., 150(2), 2009, 366–373.
[35]. H.Demiral, G. Gündüzoğlu, Removal of nitrate from aqueous solutions by activated carbon prepared from sugar beet bagasse. Bioresour. Technol., 101(6), 2010,1675–1680.
[36]. M. Arami, N.Y.Limaee, N.M. Mahmoodi, Evaluation of the adsorption kinetics and equilibrium for the potential removal of acid dyes using a biosorbent. Chem. Eng. J., 139(1), 2008, 2–10.
[37]. N.K. Soliman, A.F. Moustafa, A.A. Aboud, K.S.A. Halim, Effective utilization of Moringa seeds waste as a new green environmental adsorbent for removal of industrial toxic dyes. J. Mater. Res. Technol., 8(2),2019,1798–1808.
[38]. V.M.Vučurović,R.N.Razmovski,U.D.Miljić,V.S. Puškaš, Removal of cationic and anionic azo dyes from aqueous solutions by adsorption on maize stem tissue.J. Taiwan Inst. Chem. Eng., 45(4), 2014, 1700–1708.

Aïssatou Alioune Gaye. etal. "Bio-sorption of Methylene Blue and basic fuchsin from aqueous solution onto defatted Carica papaya seeds: mechanism and effect of operating parameters on the adsorption yield." *IOSR Journal of Environmental Science, Toxicology and Food Technology (IOSR-JESTFT)*, 13(2), (2020): pp 24-33.